# A Pyrenylpropyl Phosphonic Acid Surface Modifier for Mitigating the Thermal Resistance of Carbon Nanotube Contacts

*John H. Taphouse, O'Neil L. Smith, Seth R. Marder,* and Baratunde A. Cola**

**Efforts to utilize the high intrinsic thermal conductivity of carbon nanotubes (CNTs) for thermal transport applications, namely for thermal interface materials (TIMs), have been encumbered by the presence of high thermal contact resistances between the CNTs and connecting materials. Here, a pyrenylpropyl-phosphonic acid surface modifier is synthesized and applied in a straight forward and repeatable approach to reduce the thermal contact resistance between CNTs and metal oxide surfaces. When used to bond nominally vertically aligned multi-walled CNT forests to Cu oxide surfaces, the modifier facilitates a roughly 9-fold reduction in the thermal contact resistance over dry contact, enabling CNT-based TIMs with thermal resistances of 4.6 ± 0.5 mm$^2$ K W$^{-1}$, comparable to conventional metallic solders. Additional experimental characterization of the modifier suggests that it may be used to reduce the electrical resistance of CNT-metal oxide contacts by similar orders of magnitude.**

## 1. Introduction

With the on-going increase in the power density of electronic devices, thermal management remains a central issue for upholding device performance and reliability. Thermal interface materials (TIMs), used to conduct heat across the multiple interfaces between the device and heat sink, with unprecedentedly low thermal resistance and a high degree of mechanical compliance to accommodate mismatches in thermal expansion are required.[1] Forests comprised of nominally vertically aligned carbon nanotubes (CNTs), with individual thermal conductivities on the order of 3000 W m$^{-1}$ K$^{-1}$[2,3] and an in-plane elastic modulus as low as 8 MPa,[4] are excellent candidates for thermal interface materials (TIMs).[5–16] However, despite nearly a decade of research TIMs based on vertically aligned CNT (VACNT) forests have yet to harness effectively the high thermal conductivity of individual CNTs. One of the key obstacles that has limited the effectiveness of VACNT TIMs is the presence of high thermal contact resistances between the CNT free ends and the surfaces comprising the interface.[6–8,17] Previous approaches to mitigate the contact resistance have focused on methods for bonding the free ends of the CNTs to the interface.[6,9–14,16] A few of the more successful bonding methods that have been developed are summarized in **Table 1**. While, many of the methods have produced TIMs with thermal resistances that are comparable to conventional metallic solder TIMs (5 mm$^2$ KW$^{-1}$),[18] they are generally challenging to implement consistently, or require cumbersome processing. Specifically, Tong et al.[6] using indium to weld multiwall CNT (MWCNT) tips to glass noted that while thermal resistances on the order of 1 mm$^2$ KW$^{-1}$ were measured the thermal resistance across the entire area of the sample varied significantly, a result they attributed to inconsistent bonding at the interface. Later, Barako et al.[15] using In to bond 500 μm tall MWCNTs to glass was able to obtain thermal resistances as low as 28 mm$^2$ KW$^{-1}$. Several authors[10,11,13] have coated both MWCNT tips and the surface of the interface with films of Au and diffusion bonded the MWCNT tips under high temperature and pressure to produce resistances as low as ~4 mm$^2$ KW$^{-1}$. However, unlike bonding with In or other solders Au does not melt and reflow during the bonding process and is instead restricted to diffusing between contacting surface asperities, limiting the contact area and making it difficult to achieve adequate bonding. As stated by Wasniewski et al.,[13] Au diffusion bonding "results proved very difficult to replicate; challenges with achieving strong, uniform diffusion bonds... precluded positive test results." Ni et al.[14] reported achieving thermal resistances as low as 1.4 mm$^2$ KW$^{-1}$, by modifying and bonding CNT films with the polymer HLK5. However, some important experimental details, including the CNT forest thickness, CNT chemical modification procedure, bonding procedure, and measurement uncertainty analysis were absent from this report, therefore it was not included in Table 1. The remaining approaches summarized in Table 1 similarly produced either relatively high thermal resistances (over 5 mm$^2$ KW$^{-1}$),

J. H. Taphouse, Prof. B. A. Cola
G. W. Woodruff, School of Mechanical Engineering
Georgia Institute of Technology
Atlanta, GA, 30332–0001, USA
E-mail: cola@gatech.edu
O. L. Smith, Prof. S. R. Marder
School of Chemistry and Biochemistry
Georgia Institute of Technology
Atlanta, GA, 30332–0001, USA
E-mail: seth.marder@chemistry.gatech.edu
Prof. S. R. Marder, Prof. B. A. Cola
School of Materials Science and Engineering
Atlanta, GA, 30332–0001, USA

DOI: 10.1002/adfm.201301714

**Table 1.** Thermal resistances of bonded CNT thermal interfaces compared to conventional TIMs.

| Interface | CNT Forest Height [μm] | Measurement Pressure [kPa] | Thermal Resistance [$mm^2$ K $W^{-1}$] | Implementation Process |
|---|---|---|---|---|
| **Bonded CNT Forests:** | | | **Bonded/Dry Contact:** | |
| Si-MWCNT-In-$SiO_2$[6] | 10 | 0 | ~1/11 | Metal Evaporation, Bonding (Pressure NA[a]), 180 °C) |
| Si-MWCNT-Pd-Ag[12] | 20 | 34 | 11/22 | Drop Casting, Bonding (273 kPa, 250 °C) |
| Si-MWCNT-Au-Ag[11] | 30 | 0 | 4.5 ± 0.5/NA[a]) | Metal Evaporation, Bonding (Pressure NA[a]), 220 °C) |
| Si-Au-Patterned MWCNT-Au-Si[10] | ~60 | 63 | 62/336[b]) | Metal Evaporation, Bonding (63 kPa, 150 °C) |
| Si-MWCNT-Polymer-Ag[16] | 10–115 | 7 | 5–44/20–80 | Spray Coating, Bonding (138 kPa, RT[c]) |
| Si-MWCNT-Al/Ni-$SiO_2$[15] | 500 | 200–500 | 15–50/~1000 | Bonding (100 kPa) |
| Si-MWCNT-In-$SiO_2$[15] | 500 | 100–600 | 28–71/~1000 | Bonding (100 kPa, 180 °C) |
| Cu-MWCNT-Si[9] | NA | 0 | 10/50 | Spin Coating, Microwave Bonding (6.425 GHz, 750 kPa, 160 °C) |
| **This Work:** | | | **Bonded/Dry Contact:** | |
| Si-MWCNT-PyprPA-Cu-Ag | 15 | 7 | 4.6 ± 0.5/40 ± 20 | Solution Bath, Bonding (300 kPa, RT[c]) |
| **Conventional Materials:** | | | | |
| Greases[36] | | | 10 | |
| Gels[36] | | | 8 | |
| Phase Change[36] | | | 10 | |
| Solder[18] | | | 5 | |

[a]NA: Data not available; [b]The reported area specific thermal resistances were recalculated using the total area of the interface (4 $mm^2$) instead of only the patterned CNT area (1.13 $mm^2$) to reflect the effective thermal resistance, as would be experienced by real device; [c]RT: Room temperature.

and/or required processing that could not be scaled in a practical manner. The method developed by Lin et al.[9] to chemically modify and anchor MWCNTs to Si substrates includes spin coating followed by a two-stage microwave bonding process lasting 1.5 hours with a peak temperature and pressure of 160 °C and 750 kPa respectively. As such, there is a significant need for a method of bonding CNT free ends that can repeatedly produce low thermal contact resistances uniformly over device areas, 1–4 $cm^2$, with minimally harsh and scalable processing. Here we show that a simple organic surface modifier, a pyrenylpropyl phosphonic acid, can be synthesized and applied in a straightforward approach to consistently reduce the thermal resistance of MWCNT contacts by approximately 9-fold.

The bifunctional interface modifier was designed such that it was terminated at one end with a pyrene moiety that is known to associate with CNT sidewalls through $\pi$–$\pi$ stacking interactions.[19,20] The opposite end of the molecule is terminated with a phosphonic acid functionality, which has been shown to form robust covalent bonds to native metal oxide surfaces[21–25] that are commonplace in electronic device architectures. The effectiveness of this approach was investigated by determining the thermal resistance of nominally vertically aligned MWCNT forests coupled to Cu oxide using the pyrenylpropyl phosphonic acid (PyprPA) modifier and comparing this value to that obtained for MWCNT forests in non-bonded dry contact with the oxidized surface of Cu films. In tests of multiple samples of each type, the non-bonded MWCNT forests were found to have thermal resistances of 20–60 $mm^2$ $KW^{-1}$ whereas the forests coupled with the PyprPA modifier had thermal resistances of 4–5 $mm^2$ $KW^{-1}$, attributing the PyprPA modification and coupling process to a greater than 85% reduction in the thermal resistance as well as a substantial reduction in the sample-to-sample data scatter. Further experiments suggest that the PyprPA modifier might also be utilized to reduce the electrical contact resistance of MWCNT-Cu oxide interfaces by as much as 90%, which would render it of interest for CNT interconnects and possibly even graphene-based electronic devices. The attachment strength of PyprPA coupled MWCNT forest-Cu oxide interfaces was measured through a tensile failure mode to be 290–390 kPa, of the same order as Au diffusion bonded CNT TIMs.[11]

## 2. Pyrenylpropyl Phosphonic Acid

The phosphonic acid was synthesized as illustrated in **Scheme 1** in two steps from 1-(3-iodopropyl)pyrene 1, which was obtained using the method of Gastaldi and Stien.[26] Iodide 1 was then converted to phosphonate 2 and, with subsequent hydrolysis,

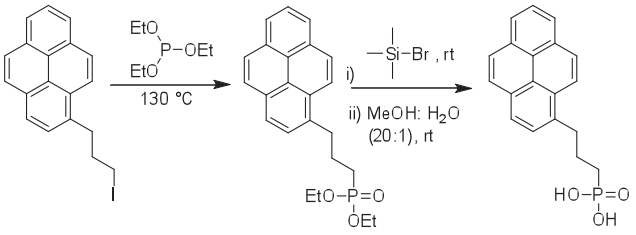


**Scheme 1.** Synthesis of pyrenylpropyl phosphonic acid. **1** iodide precursor, **2** phosphonate, and **3** phosphonic acid.

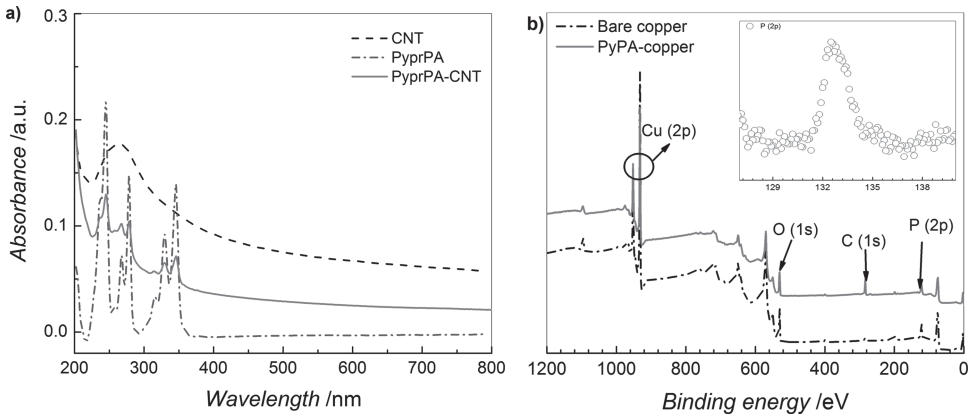


**Figure 1.** Modification of MWCNTs and copper oxide with phosphonic acid. a) Comparison of the UV-Vis spectra of the MWCNT, phosphonic acid moiety, and the modified nanotube. b) XPS survey spectra of the modified and unmodified copper substrate

to phosphonic acid 3. The ability of the phosphonic acid to successfully modify both the MWCNTs and Cu oxide surfaces was verified independently using UV–visible (UV–vis) and X-ray photoelectron spectroscopy (XPS), respectively. MWCNTs were modified with the PyprPA using a protocol similar to that outlined by Simmons et al.[27] The Cu surfaces were functionalized with the PyprPA using a protocol analogous to that reported elsewhere for the modification of indium tin oxide with phosphonic acids[25] (see experimental section and supporting information for synthetic and modification details).

UV–vis spectra demonstrating the successful modification of MWCNTs are shown in **Figure 1**a. Here the spectrum of the modified MWCNTs appears to be a superposition of the absorbance of the pristine phosphonic acid onto the MWCNT background. Calibration curves for both the pristine MWCNTs and the phosphonic acid were generated and used to estimate the amount of associated PyprPA per microgram of MWCNT ($1.2 \times 10^{-4}$ mol $\mu g^{-1}$; Figure S2). In a similar manner, XPS was used to confirm the modification of the Cu oxide substrate with the phosphonic acid and evaluate the thickness of the overlayer. Specifically, the survey spectra (Figure 1b) show an increase in the C 1s signal upon modification of the Cu oxide film with the PyprPA and the high resolution P (2p) scan shown in the inset of Figure 1b confirms the presence of phosphorus on the surface. An approach previously discussed by Wallart,[28] was used to assess the surface coverage of the modifier on the Cu oxide surface. Here the thickness of the PyprPA film was approximated to be 10.4 ± 0.3 Å which is less than the 13.6 Å calculated for a Hartree-Fock optimized geometry of a molecule that is oriented perpendicular to the surface (Figure S5). This suggests that we did not form multilayers on the Cu oxide surface after sonication in a solution of ethanol:chloroform (1:1) for 5 min to remove excess PyprPA.

## 3. Thermal Characterization

For thermal characterization the PyprPA modifier was used to couple the free tips of vertical multiwall MWCNT forests, roughly 15 µm in height with an average tube diameter of 8 nm (**Figure 2**a) (synthesis details provided in supporting information), to 300 nm thick Cu films evaporated on 25 µm Ag foil substrates (Alfa Aesar 11498). A surface oxide layer was established on the Cu films as described in the experimental section to facilitate experimental control, although the native oxide layer may be sufficient for the coupling process. The final sample configuration for thermal measurements can be seen in Figure 2b. The thermal resistance of both MWCNT forests coupled with the PyprPA and those in dry contact with oxidized Cu films was measured using a photoacoustic (PA) technique. The PA

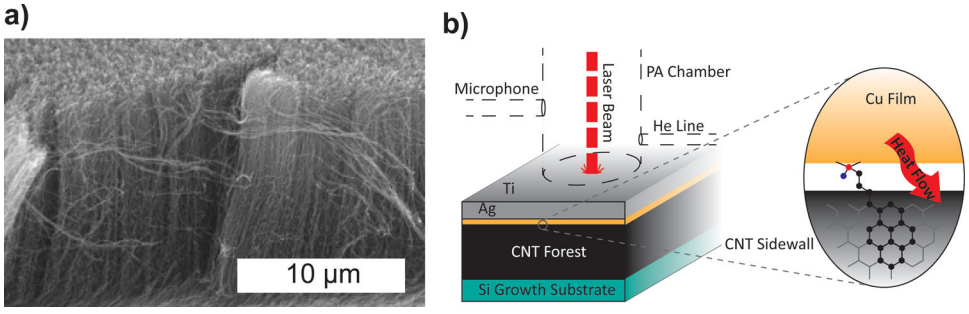


**Figure 2.** Sample and photoacoustic measurement configuration. a) Representative scanning electron micrograph of a MWCNT forest used for PyprPA interface coupling. b) Photoacoustic measurement configuration (left) used to measure the thermal resistance of MWCNT forests coupled to oxidized Cu surfaces with the PyprPA modifier (right).

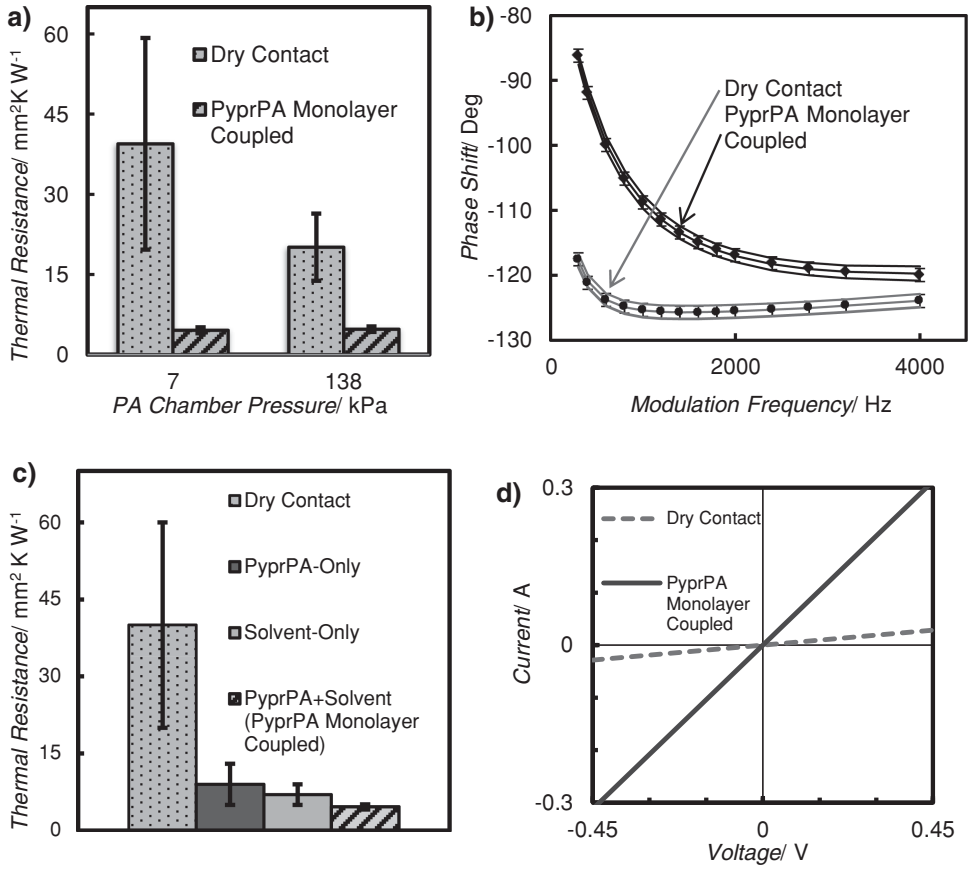


**Figure 3.** Photoacoustic characterization of MWCNT forests in dry contact and PyprPA coupled configurations. a) Coupling the MWCNT tip interface with the PyprPA modifier reduces the thermal resistance of the interface material by 85–75% on average and alleviates the pressure dependence. Error bars include measurement uncertainty and variations in thermal resistance from multiple measured samples. b) A representative photoacoustic measurement data set for a PyprPA coupled MWCNT forest, including theoretical curve fits to the data and to data sets shifted by the measurement uncertainty of ±1 degrees (solid lines). c) Effect of solvent on thermal resistance at 7 kPa. Results shown for the Solvent-Only configuration were collected before delamination occurred. d) Coupling the MWCNT tip interface with the PyprPA modifier may reduce the electrical resistance of the interface material by up to 90%.

technique is a nondestructive method for measuring the thermal conductivity of materials, including thin films, and the thermal resistance of interfaces. An overview of the technique and the underlying theory has been reported previously[7,29,30] and its application in this work is given in the Supporting Information.

The base pressure in the PA acoustic chamber, located immediately above the sample surface (Figure 2b), can be altered to examine the thermal resistance of the sample as a function of the pressure applied to it. PA tests were conducted at cell pressures of 7 kPa, a slight positive pressure to ensure that the chamber was filled with helium, and 138 kPa, to apply modest pressure to the interface. Five samples treated with the PyprPA modifier were prepared and PA tests were conducted at 3–4 different locations on each sample, providing 16 total measurements. Similarly, four dry contact samples were prepared and measurements were taken at 2–3 different locations on each sample, providing 11 total measurements. The beam diameter at the sample surface was approximately 1 mm and the surface area of each sample was 1 $cm^2$. By testing 2–4 different locations on the surface of each sample the efficacy of the coupling procedure over device-sized areas was examined. The total thermal resistance, comprised of the sum of the contact resistance at the MWCNT tip-Cu interface, the resistance of the MWCNT forest, and the contact resistance at the MWCNT-Si growth substrate interface, for both sample configurations and both PA chamber pressures is displayed in **Figure 3**a. The error in the measurement has contributions from both the resolution of the experimental setup and variations in thermal resistance from sample to sample.

The total thermal resistance of the dry contact samples was measured to be 40 ± 20 and 20 ± 6 $mm^2$ $KW^{-1}$ at pressures of 7 and 138 kPa, respectively. Analogous trends have been observed in previous studies[10,31] and were analyzed theoretically by Cola et al.[32] In essence, increasing the pressure applied to the interface compresses the MWCNT forest and brings additional MWCNTs into contact with the Cu surface in addition to increasing the contact length of MWCNTs already in contact with the surface. The net effect is an increase in the contact area, or the area available for heat conduction, resulting in a decrease in the thermal contact resistance.

The total thermal resistance of the samples coupled with a monolayer of the PyprPA modifier using the procedure

outlined in the experimental section was measured to be 4.6 ± 0.5 and 4.9 ± 0.5 $mm^2$ $KW^{-1}$ at pressures of 7 and 138 kPa respectively. The PyprPA modification and coupling procedure reduced the thermal resistance of the MWCNT forest by 88%-76% on average. The fact that the thermal resistance of the coupled samples did not exhibit a significant dependence on pressure, over the range considered, suggests that the contact area is constant and that the interface is well bonded. Moreover, the low thermal resistances achieved by coupling were consistent across the entire area of the sample (1 $cm^2$) demonstrating the strong uniform bonding over device-sized areas. Three additional PyprPA-coupled samples were fabricated in which the PyprPA:CuO was not sonicated prior to coupling this surface to the MWCNT forest. This was done to assess whether steps to attempt to create only a monolayer of PyprPA at the interface were required. The thermal resistance of the samples without sonication prior to MWCNT coupling were measured to be 9 ± 6 and 7 ± 3 $mm^2$ K $W^{-1}$ at PA chamber pressures of 7 and 138 kPa respectively, which is an approximately 45% increase in the thermal resistance over MWCNT forests coupled to sonicated PyprPA:CuO substrates at 7 kPa. This increase in resistance can be attributed to the disorder and weak bonding associated with multiple layers of PyprPA not removed by the sonication step before coupling the surface to MWCNTs.

For all of the aforementioned MWCNT-PyprPA:CuO samples the MWCNT forest was wet with a few drops of solvent (ethanol:chloroform (1:1)) and subsequently dried during the coupling process. It has been previously suggested that capillary forces present during the drying process may drive MWCNTs towards the PyprPA:CuO surface and enhance the contact area.[16] To elucidate the role of solvent in the MWCNT-PyprPA:CuO coupling process two additional sample types were fabricated. For the first type (PyprPA-only) the sample was fabricated following the same PyprPA:CuO-sonication-MWCNT coupling procedure except no solvent was dripped onto the top of the MWCNT forest to wet the interface beforehand. For the second type (solvent-only) the CuO film was not modified with PyprPA prior to the coupling process. The thermal resistance of two PyprPA-only samples was measured to be 9 ± 4 and 8 ± 2 $mm^2$ $KW^{-1}$ at 7 and 138 kPa, respectively (Figure 4c). Likewise, two solvent-only samples were prepared and the thermal resistance was measured to be 7 ± 2 $mm^2$ $KW^{-1}$ at 7 kPa and 7 ± 1 $mm^2$ $KW^{-1}$ at 138 kPa the first time each sample was characterized using PA. However, the MWCNT-CuO interface was observed to be very weakly adhered. As such, when the solvent-only samples were removed and reinserted into the PA setup to measure the thermal resistance at a different location on the sample the MWCNT-CuO interface delaminated and the thermal resistance was measured to increase. After full delamination of the MWCNT-CuO interface the thermal resistance was measured to be approximately 19 ± 1 and 11 ± 1 $mm^2$ $KW^{-1}$ at 7 and 138 kPa respectively.

The exact contributions of the PypPA modifier and solvent cannot be resolved from these results; yet it is clear that both the solvent and PyprPA modifier play significant and different roles in decreasing the thermal resistance of the interface. For the PyprPA-only samples the thermal resistance was roughly 22% reduced from the dry contact samples at 7 kPa. This demonstrates a significant benefit to having stronger covalent interactions between the phosphonic acid and the Cu oxide and $\pi$–$\pi$ stacking interactions between the pyrenyl group and the MWCNT forest mediated by the PyprPA modifier, as compared to only having van der Waals interactions in the dry contact arrangement. The notion that interfacial heat transfer can be enhanced by improving the strength of bonding at the interface is well accepted,[32,33] although it has only recently been observed for surface modifiers experimentally.[34] It should however be noted that without direct knowledge of the contact area at the interface it remains unclear if the reduction in thermal resistance of the PyprPA-only samples can be entirely attributed to enhanced bond strength as a result of the modifier. For the solvent-only interfaces the thermal resistance was 18% less than dry contact samples at 7 kPa before delamination occurred. This suggests that capillary forces during the drying process do in fact pull MWCNTs towards the CuO surface and considerably increase the contact area. It has recently been demonstrated that solvent wetting of the van der Waals interactions between nanostructures can reduce boundary phonon scattering and enhance the nanostructures thermal conductivity.[35] However, it is unlikely that the solvent influences thermal transport within the CNT forest in a manner that would significantly reduce the total thermal resistance, especially for forests as short as the ones used in this study, as several prior studies have shown that the total thermal resistance of CNT interfaces is dominated by the contact resistances.[5–7] After routine handling the van der Waals bonded MWCNT-CuO interface of the solvent-only samples delaminated causing the thermal resistance of the samples to increase, whereas all samples coupled with the PyprPA remained adhered further demonstrating the benefit of the stronger covalent and $\pi$–$\pi$ bonding present with the modifier.

## 4. Thermal Stability, Attachment Strength, and Electrical Characterization

To further assess the utility of the MWCNT-PyprPA:CuO system for thermal and electrical applications the thermal stability of the PyprPA molecule, and the attachment strength and current-voltage characteristics of MWCNT-PyprPA:CuO interfaces were examined. Thermal stability of the MWCNT-PyprPA:CuO interface was studied using thermogravimetric analysis (TGA) (Figure S3b) and showed approximately a 22 wt% loss that commenced at around 200 °C, well above the typical operating temperatures of electronic devices. The attachment strength of the PyprPA coupled samples used in PA tests (3 total) was measured through a tension failure mode (Figure S6) to be 340 ± 50 kPa, which is of similar order to the strength of Au-Au diffusion bonded MWCNT forest interfaces.[11] All samples failed at the PyprPA:CuO interface and no appreciable differences in attachment strength were observed between all three PyprPA coupled interface configurations (i.e., solvent, with and without sonication, and dry coupled interfaces). Samples for current-voltage scans were fabricated by growing MWCNTs on electrically conductive Cu substrates and coupling them to PyprPA:CuO films. Current-voltage scans were conducted using a 2-probe technique by contacting the Cu growth substrate and modified Cu surface (Figure S7). As

such the measurement includes contributions from the oxidized Cu film, MWCNT forest, Cu growth substrate and all intermediate interfaces; hence, it is not meaningful to extract the resistance from this data. Furthermore, the measurement is sensitive to the separation distance between the probes and the pressure applied to them. Care was taken to place the probes as consistently as possible; however, it was not precisely controlled. Coupling the MWCNT tip interface with a monolayer of PyprPA reduced the total electrical resistance by approximately 90% over dry contact. The reduction in electrical resistance was approximately 85% for samples that were not sonicated to facilitate the presence of a monolayer of PyprPA in the interface (see Figure S7). All PyprPA coupled interfaces displayed a linear relationship, suggestive of ohmic behavior, over the scan range from –0.45 to + 0.45 V as shown in Figure 4d and therefore might be useful for CNT interconnects.

## 5. Conclusions

We have synthesized a pyrene-propyl phosphonic acid modifier for coupling CNTs to metal oxide surfaces in a simple and scalable manner to reduce the thermal contact resistance. When used to couple vertical MWCNT forests to oxidized Cu surfaces the PyprPA modifier reduced the thermal contact resistance by approximately 9-fold over MWCNT forests in non-bonded dry contact. As a thermal interface material PyprPA coupled MWCNT forests had a thermal resistance of 4.6 ± 0.5 $mm^2$ $KW^{-1}$, which is on par with the resistance of conventional thin-film metallic solders.[18] Electrical characterization of PyprPA coupled and dry contact CNT interfaces indicate that the modifier may reduce the electrical contact resistance by a similar magnitude. The results of this work suggests that surface modifiers such as the one synthesized here could be used with relatively simple and repeatable processing steps to reduce contact resistances in CNT based architectures for thermal and electrical transport.

## 6. Experimental Section

*Pyrenylpropyl Phosphonic Acid Synthesis*: The phosphonic acid was synthesized over two steps from 1– (3-iododpropyl)pyrene which was obtained using the method of Gastaldi and Stien.[26] The iodide (1.35 g, 3.65 mmol) was heated with triethylphosphite (1.82 g, 10.94 mmol) at 130 °C overnight. Excess triethylphosphite and other volatiles were removed under vacuum (approximately 20 mTorr) with heating (100 °C) to give waxy solid (798 mg, 57% yield). $^1$H-NMR (300 MHz, $CDCl_3$): $\delta$ 8.27 (d, $J$ = 9 Hz, 1H), 7.97–8.18 (m, 7H), 7.86 (d, $J$ = 89 Hz, 1H), 4.02–4.13 (m, 4H), 3.45 (t, $J$ = 6 Hz, 2H), 2.14–2.23 (m, 2H), 1.88 (m, 2H), 1.29 (t, $J$ = 7.5 Hz, 6H).). $^{13}$C{$^1$H} NMR (75.5 MHz, $CDCl_3$) $\delta$ 135.31, 135.30, 131.38, 130.84, 130.00, 128.69, 127.46, 127.42, 127.33, 126.75, 125.85, 125.07, 124.95, 124.79, 124.78, 123.4, 61.52 (d, $J$ = 6.04 Hz), 33.95 (d, $J$ = 16 Hz), 25.42 (d, $J$ = 145.7 Hz), 24.51, 16.46 (d, $J$ = 5.3 Hz). $^{31}$P{$^1$H} NMR (162 MHz, $CDCl_3$) $\delta$ 32.6. Anal. Calcd for $C_{23}H_{25}O_3P$: C, 72.62; H, 6.62. Found: C, 72.36; H, 6.76. HRMS (m/z) $[M]^+$ Calcd for $C_{23}H_{25}O_3P$: 380.1534. Found, 380.1541. The phosphonic acid was obtained by dissolving the phosphonate (0.38 g, 1 mmol) in dry dichloromethane and adding bromotrimethylsilane (0.46 g, 3 mmol) dropwise. The solution was stirred overnight. The volatiles were then removed by rotary evaporation after which a methanol: water solution (20:1) was added to the residue and the contents of the flask were stirred overnight. The reaction mixture was then concentrated by rotary evaporation to give a solid. The solid was washed with methanol and dried under vacuum to give an off-white powder (144 mg, 44% yield). $^1$H-NMR (300 MHz, DMSO): $\delta$ 8.37 (d, $J$ = 9 Hz, 1H), 8.02–8.28 (m, 7H), 7.94 (d, $J$ = 9 Hz, 1H), 3.40(t, $J$ = 7.5 Hz, 2H), 3.37–3.41(m, 2H), 1.66 (p, $J$ = 9Hz, 2H). $^{13}$C {$^1$H} NMR (75.5 MHz, DMSO): $\delta$ 136.44, 130.90, 130.42, 129.32, 128.16, 127.65, 127.47, 127.26, 126.54, 126.15, 124.96, 124.93, 124.81, 124.24, 124.15, 123.55, 33.3 (d, $J$ = 16 Hz), 27.41 (d, $J$ = 140 Hz), 25.63 (d, $J$ = 4.5 Hz). $^{31}$P{$^1$H} NMR (162 MHz, DMSO): $\delta$ 27.91. Anal. Calcd for $C_{19}H_{17}O_3P$: C, 70.37; H 5.28. Found: 70.63; 5.26. HRMS (m/z): $[M]^+$ calcd for $C_{19}H_{17}O_3P$: 324.0915; found, 324.0915.

*Interface Coupling Procedure*: Before modification took place the as-evaporated Cu films were exposed to an $O_2$ plasma at 200 mTorr pressure for 2 min to facilitate formation of a consistent surface oxide layer. Upon removal from the plasma chamber the Cu films were immediately placed in a 1.5 mM solution of the PyprPA modifier in ethanol:chloroform (1:1). The Cu films were soaked for at least 1 day, during which time the modification took place. The minimum soak time required to form a monolayer was not explored. For coupling the MWCNT forests, the PyprPA-modified Cu oxide film (PyprPA:CuO) was removed from the PyprPA solution and sonicated in a solution of ethanol:chloroform (1:1) for 5 min to remove excess PyprPA with the intent of leaving only a monolayer covalently bonded to the Cu oxide surface. The top of the MWCNT forest was then wetted with a few droplets of ethanol:chloroform (1:1) and the PyprPA:CuO film was placed onto the wet forest. 300 kPa of pressure was applied to the still wet interface and it was allowed to dry for at least 5 hours at room temperature.

## Supporting Information

Supporting Information is available from the Wiley Online Library or from the author.

## Acknowledgements

J. H. Taphouse and O. L. Smith contributed equally to this work. This work was supported in part by the Center for Interface Science: Solar Electric Materials, an Energy Frontier Research Center funded by the U.S. Department of Energy, Office of Science, Office of Basic Energy Sciences under Award Number DE-SC0001084 (O.L.S.) and National Science Foundation Award No. CBET 1133071 (J.H.T.). We also thank Georgia Power (S.R.M.) and the George W. Woodruff School (B.A.C.) for support. We thank Dr. Asha Sharma for performing current-voltage scans, Justin J. Nguyen for help with CNT growth, and Parisa Pour Shahid Saeed Abadi for aiding in tensile tests.

Received: May 20, 2013
Revised: July 3, 2013
Published online: September 4, 2013

[1] International Technology Roadmap for Semiconductors, **2012**: www.ITRS.net/home.html, accessed: May, 2012.
[2] P. Kim, L. Shi, A. Majumdar, P. L. McEuen, *Phys. Rev. Lett.* **2001**, *87*.
[3] E. Pop, D. Mann, Q. Wang, K. E. Goodson, H. J. Dai, *Nano Lett.* **2006**, *6*, 96–100.
[4] Y. Won, Y. Gao, M. A. Panzer, S. Dogbe, L. Pan, T. W. Kenny, K. E. Goodson, *Carbon* **2012**, *50*, 347–355.
[5] X. J. Hu, A. A. Padilla, J. Xu, T. S. Fisher, K. E. Goodson, *J. Heat Transfer* **2006**, *128*, 1109–1113.
[6] T. Tong, Y. Zhao, L. Delzeit, A. Kashani, M. Meyyappan, A. Majumdar, *IEEE Trans. Compon. Packag. Technol.* **2007**, *30*, 92–100.

[7] B. A. Cola, J. Xu, C. R. Cheng, X. F. Xu, T. S. Fisher, H. P. Hu, *J. Appl. Phys.* **2007**, *101*, 054313.
[8] M. A. Panzer, H. M. Duong, J. Okawa, J. Shiomi, B. L. Wardle, S. Maruyama, K. E. Goodson, *Nano Lett.* **2010**, *10*, 2395–2400.
[9] W. Lin, R. W. Zhang, K. S. Moon, C. P. Wong, *Carbon* **2010**, *48*, 107–113.
[10] A. Hamdan, J. Cho, R. Johnson, J. Jiao, D. Bahr, R. Richards, C. Richards, *Nanotechnology* **2010**, *21*, 015702.
[11] R. Cross, B. A. Cola, T. Fisher, X. F. Xu, K. Gall, S. Graham, *Nanotechnology* **2010**, *21*, 445705.
[12] S. L. Hodson, T. Bhuvana, B. A. Cola, X. F. Xu, G. U. Kulkarni, T. S. Fisher, *J. Electron. Packag.* **2011**, *133*, 020907.
[13] J. R. Wasniewski, D. H. Altman, S. L. Hodson, T. S. Fisher, A. Bulusu, S. Graham, B. A. Cola, *J. Electron. Packag.* **2012**, *134*, 020901.
[14] Y. X. Ni, H. L. Khanh, Y. Chalopin, J. B. Bai, P. Lebarny, L. Divay, S. Volz, *Appl. Phys. Lett.* **2012**, *100*,193118.
[15] M. T. Barako, Y. Gao, A. M. Marconnet, M. Asheghi, K. E. Goodson, at 13th Ieee ITherm, San Diego, **2012**.
[16] J. H. Taphouse, T. L. Bougher, V. Singh, P. P. Abadi, S. Graham, B. A. Cola, *Nanotechnology* **2013**, *24*, 105401.
[17] J. K. Yang, Y. Yang, S. W. Waltermire, T. Gutu, A. A. Zinn, T. T. Xu, Y. F. Chen, D. Y. Li, *Small* **2011**, *7*, 2334–2340.
[18] D. D. L. Chung, *Appl. Therm. Eng.* **2001**, *21*, 1593–1605.
[19] S. G. Stepanian, V. A. Karachevtsev, A. Y. Glamazda, U. Dettlaff-Weglikowska, L. Adamowicz, *Mol. Phys.* **2003**, *101*, 2609–2614.
[20] Q. Yang, L. Shuai, J. Zhou, F. C. Lu, X. J. Pan, *J. Phys. Chem. B* **2008**, *112*, 12934–12939.
[21] P. H. Mutin, G. Guerrero, A. Vioux, *Comptes Rendus Chimie* **2003**, *6*, 1153–1164.
[22] P. H. Mutin, G. Guerrero, A. Vioux, *J. Mater. Chem.* **2005**, *15*, 3761–3768.
[23] P. Kim, N. M. Doss, J. P. Tillotson, P. J. Hotchkiss, M. J. Pan, S. R. Marder, J. Y. Li, J. P. Calame, J. W. Perry, *ACS Nano* **2009**, *3*, 2581–2592.
[24] P. J. Hotchkiss, M. Malicki, A. J. Giordano, N. R. Armstrong, S. R. Marder, *J. Mater. Chem.* **2011**, *21*, 3107–3112.
[25] S. A. Paniagua, P. J. Hotchkiss, S. C. Jones, S. R. Marder, A. Mudalige, F. S. Marrikar, J. E. Pemberton, N. R. Armstrong, *J. Phys. Chem. C* **2008**, *112*, 7809–7817.
[26] S. Gastaldi, D. Stien, *Tetrahedron Lett.* **2002**, *43*, 4309–4311.
[27] T. J. Simmons, J. Bult, D. P. Hashim, R. J. Linhardt, P. M. Ajayan, *ACS Nano* **2009**, *3*, 865–870.
[28] X. Wallart, C. H. de Villeneuve, P. Allongue, *J. Am. Chem. Soc.* **2005**, *127*, 7871–7878.
[29] H. P. Hu, X. W. Wang, X. F. Xu, *J. Appl. Phys.* **1999**, *86*, 3953–3958.
[30] X. Wang, B. A. Cola, T. L. Bougher, S. L. Hodson, T. S. Fisher, X. Xu, in *Annual Review of Heat Transfer,* Begell House, Redding Connecticut USA **2013**, pp.135–157.
[31] B. A. Cola, X. F. Xu, T. S. Fisher, *Appl. Phys. Lett.* **2007**, *90*, 093513.
[32] B. A. Cola, J. Xu, T. S. Fisher, *Int. J. Heat Mass Transfer* **2009**, *52*, 3490–3503.
[33] R. Prasher, *Appl. Phys. Lett.* **2009**, *94*, 041905.
[34] M. D. Losego, M. E. Grady, N. R. Sottos, D. G. Cahill, P. V. Braun, *Nat. Mater.* **2012**, *11*, 502–506.
[35] J. K. Yang, Y. Yang, S. W. Waltermire, X. X. Wu, H. T. Zhang, T. Gutu, Y. F. Jiang, Y. F. Chen, A. A. Zinn, R. Prasher, T. T. Xu, D. Y. Li, *Nat. Nanotechnol.* **2012**, *7*, 91–95.
[36] R. Prasher, *Proc. IEEE* **2006**, *94*, 1571–1586.